

Performance-Based Seismic Assessment of Shallow Tunnels using Pushover Analysis

Mahan Pasdarpour*, Shahram Vahdani²

1. PhD Student of Geotechnical engineering, University of Texas at Arlington, USA
2. Assistant Professor of Civil Engineering, University of Tehran, Tehran, Iran

Received: 27 Jul 2013; Accepted: 30 Dec 2014
DOI: 10.22044/TUSE.2015.376

Keywords

Dynamic Analysis
FEMA 302
Ovaling/Racking
Performance Point
Pushover Analysis
Linings of Shallow Tunnels
Standard Acceleration Response Spectrum

Extended Abstract

This paper aims to use pushover analysis for performance-based seismic assessment of linings of shallow tunnels constructed in soil that are subjected to vertical shear waves. Pushover analysis is a nonlinear static analysis that works based on pushing laterally two-dimensional (2D) numerical nonlinear model of soil with tunnel statically. This analysis considers just ovaling/racking deformation of a lining and compared to the other existing seismic analysis approaches, it has the advantage of using directly a standard acceleration response spectrum as seismic demand. Initially in this paper, responses of a typical tunnel due to four earthquakes were calculated using pushover analysis. Then, the approach of employing a typical standard acceleration response spectrum as seismic demand was presented using the building standard spectrum of FEMA 302 provisions. All the resultant performance points of pushover analyses were then evaluated by carrying out nonlinear dynamic time history analyses and the method was verified. However, further studies are required to propose an acceptable response spectrum for the geotechnical nature of soil deposits containing shallow tunnels as their seismic demand.

This paper aims to use pushover analysis for performance-based seismic assessment of linings of shallow tunnels constructed in soil that are subjected to vertical shear waves. Pushover analysis is a nonlinear static analysis that works based on pushing laterally two-dimensional (2D) numerical nonlinear model of soil with tunnel statically. This analysis considers just ovaling/racking deformation of a lining and

1. Introduction

Seismic evaluation of underground structures is so different from structures on the ground because of their interaction with surrounding soil. A tunnel lining undergoes three primarily modes of deformation during seismic shaking: Ovaling/Racking, axial and curvature deformation (FHWA, 2009). The ovaling/racking deformation, caused by seismic waves propagating perpendicular to the tunnel longitudinal axis, is the argument of this paper. This deformation occurs in the plane of the tunnel cross section (Owen and Scholl 1981). Moreover, among variety of the seismic waves such as the Rayleigh wave, the vertically propagating shear wave (SV-wave) is generally considered as the most critical one for this mode of deformation (Wang 1993). There are two main types of seismic design approaches for assessing a tunnel linings

ovaling/racking deformation induced by SV-waves: a) Free-field racking deformation methods and b) Soil-structure interaction approaches (Hashash 2001). The former one does not consider soil-lining interaction in estimating and applying seismic demand unlike the latter one and is not of great attention nowadays.

Soil-structure interaction approaches have been classified in many ways. Here is a new classification of them including three types: a) Dynamic earth pressure methods, b) Simplified Ovaling/Racking coefficient methods and c) Numerical methods. Mononobe-Okabe method is the most famous one among the first type of approaches (Seed and Whitman 1970). These methods are just for cut-and-cover rectangular cross-sections and generally, it is not recommended to use them due to their unrealistic results. In the second category, a demand free-field racking deformation is multiplied by a

* The University of Texas at Arlington; Department of Civil Engineering; 425 Nedderman Hall; 416 Yates St.; Box 19308; Arlington; TX 76019; Phone: 817-272-2201; Fax: 817-272-2630; Email: mahan.pasdarpour@gmail.com

coefficient representing soil-structure interaction effect obtained from analytical or numerical solution. For instance, Wang (1993) and Penzien (2000) presented an elastic analytical solution for deep circular and shallow rectangular tunnels. Furthermore, Huo et al. (2006) presented analytical solution for deep rectangular tunnel. However, for non-circular and non-rectangular tunnels or inelastic conditions, a closed form or a general numerical solution for estimating soil-structure interaction coefficient is not available; hence, numerical methods as the third approach are vital in such cases. In FHWA (2009), three numerical approaches have been introduced: 1) Pseudo static seismic coefficient method, 2) Pseudo dynamic time history analysis and 3) Dynamic time history analysis. Although, these approaches and other similar numerical approaches are not restricted to the shape and depth of tunnels, none of them is able to use directly a target standard acceleration response spectrum as seismic demand.

However, what does it mean to use a target standard acceleration response spectrum for seismic analysis of a tunnel lining? A building DBL standard acceleration response spectrum (Such as FEMA 302¹ building spectrum) can predict the seismic response of it due to a design base level earthquake. On the other hand, the model of soil containing tunnel (see Figure 2) can be like a building and seismic response of this model (such as acceleration on the ground) due to a standard earthquake can be predicted using its own standard acceleration response spectrum. If the whole model of soil including the tunnel acts as a building, the tunnel lining represents a beam in that building, and by calculating the building response, hence, the seismic response of the beam is obtained. The problem is that whether it is possible to summarize behavior of any soil deposits in several standard spectra as what we do for buildings, which we presumed it would be possible.

Nevertheless, what is the advantage of pushover numerical analysis using a typical soil deposit standard spectrum in seismic design of tunnel lining? The justification of using a standard spectrum by pushover analysis in tunnel design case is exactly similar to a building case, so that

in all current numerical approaches for tunnels, seismic demand comes from set of earthquakes or a peak ground acceleration corresponding to desired level of seismic hazard, where both have their own disadvantages. Use of a set of earthquakes in dynamic analysis, alongside being time-consuming, is also a controversial problem because different set of earthquakes will lead to different results. Furthermore, a peak ground acceleration coming from a seismic hazard analysis does not have the effect of tunnel presence in its determination. It should be noted that tunnel presence will influence the ground fundamental period and nonlinear behavior of its surrounding soil simultaneously, which these two factors affect peak ground acceleration in turn. Moreover, performing site response analysis (e.g. in Shake2000) using again set of earthquakes to extract ground maximum acceleration or displacement profile for applying to a numeric model has both two previous problems together. However, using a standard spectrum is timely efficient and does not have much variance unlike set of earthquakes. Given the above facts, a new nonlinear static analysis is needed to be able to both employ a standard spectrum and account for tunnel presence (nonlinear soil-structure interaction) in calculation of seismic demand. In order to achieve this new numerical analysis method, concepts of conventional pushover analysis for buildings (Krawinkler 1998 and Chopra 2002) and common pseudo static numerical linear analysis for tunnels (Hashash et al., 2001) are combined together. The pushover analysis, comprising nonlinearity and being static, is a technical way, which is effective for using a typical standard spectrum in calculation of linings internal forces and deformations due to ovaling/racking deformations induced by SV-waves.

In pushover analysis of buildings, one numerical nonlinear static analysis replaces several rigorous time history analyses for seismic design or rehabilitation. This analysis has different types (e.g. dynamic pushover, modal pushover, etc.), but two conventional types of the analysis include target displacement methods (FEMA 356 2000) and capacity spectrum methods (ATC 40 1996) that the latter one was

¹ NEHRP Recommended Provisions for Seismic Regulation of New Buildings and Other Structures

used in this paper to assess the seismic performance of shallow tunnels. A summary of capacity spectrum method for seismic analysis of a building is illustrated in Figure 1, and we intend to develop it to tunnels. According to Figure 1, the seismic capacity curve is acquired by applying an incremental progressive lateral load to the nonlinear model of a building and drawing the diagram of base shear force versus roof displacement. In order to intersect capacity with a demand, which is for a SDOF (Single Degree Of Freedom) system, it is necessary to convert the diagram of base shear-roof displacement to its equivalent SDOF system diagram considering only the fundamental mode of vibration. By dividing base shear of equivalent SDOF system to its mass, capacity curve will be calculated in terms of roof acceleration versus roof displacement. On the other hand, the seismic demand curve is

usually a standard acceleration response spectrum from a seismic design manual (e.g. FEMA 450), which corresponds a target seismic hazard level. In the next step, a performance point will be guessed on the capacity curve and according to it; a damping coefficient will be calculated indicating the intensity of buildings nonlinear behavior. Afterward, the seismic demand curve will be reduced based on the calculated damping coefficient. Eventually, by intersecting the capacity curve and the reduced demand curve, there would be an intersection point resultantly. If the intersection point is equal to our primarily guessed performance point, then this point will be the correct performance point; otherwise, another performance point must be guessed and the interacting procedure may be repeated until reaching a satisfactory convergence.

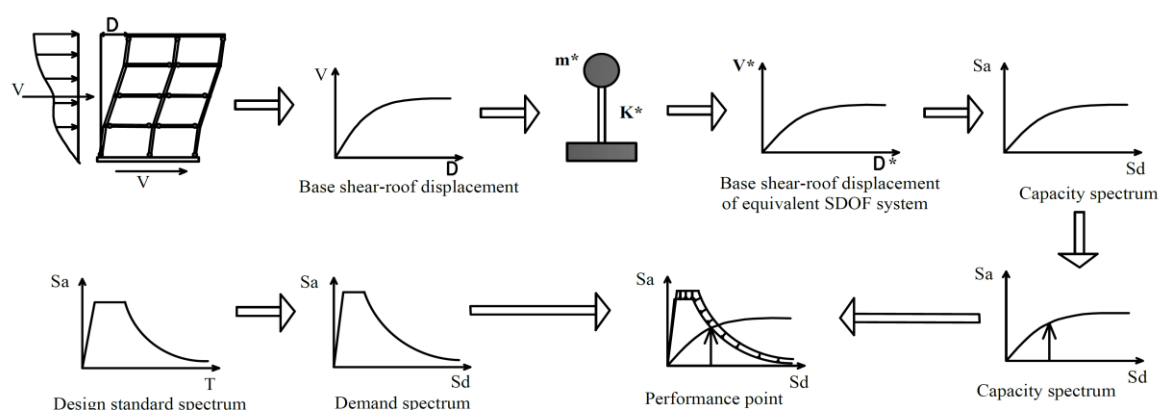


Figure 1: Conventional pushover analysis using the capacity spectrum method for buildings

In section 2.1, the new pushover analysis method was developed for shallow tunnels using four earthquakes. In order to develop, conditions of shallow tunnel in soil were chosen because underground structures constructed in either shallow depth or soil environment can be expected to suffer more damages compared to openings constructed in depth or rock (Power et al., 1998). Moreover, according to the following pushover analysis, the equations are reliable for near ground surface due to the model boundary conditions during pushing process. It is better to assume shallow tunnels as the ones constructed within approximate overburden depth of one up to two times of their heights. In section 2.2, due to lack of

standard acceleration response spectrum for soil deposit in technical literature, the building standard spectrum of FEMA 302 was utilised for pushover analysis of tunnel. In section 3, the obtained pushover results of section 2 were, then, compared by nonlinear time history analyses.

2. Seismic assessment of shallow tunnels using pushover analysis

Initially in part 2.1 of this section, the conventional pushover analysis of buildings was developed for seismic assessment of shallow tunnels using accelerograms of earthquakes as seismic demand. Afterward, in part 2.2, the procedure of the same

pushover analysis was adapted for using a standard spectrum demand.

2.1. Pushover analysis using an earthquake demand

The pushover analysis method for tunnels using an earthquake demand has been summarized in nine steps as followed in current section. Performing these nine steps will lead to tunnel linings internal forces and deformations due to its ovaling/racking deformation for a target seismic excitation. In this section, four earthquakes have been used as seismic excitation (demand) sources and amount of deformations of tunnel linings due to each one of these earthquakes have been obtained as the results of pushover analyses.

Step 1: Modeling

A two-dimensional (2D) plain strain box of soil was modeled using finite-element method (FEM), which contains a shallow three-arch tunnel as shown in Figure 2. This kind of tunnel has three arches with different radii in its cross-section geometry similar to what is seen in Figure 3. As a nonlinear analysis, both tunnel and soil can be inelastic but in this paper, tunnel was assigned elastically and soil was modeled with Mohr-Coulomb failure criteria. Tunnel lining details have been illustrated in Figure 3 and Table 1. Furthermore, model initial dimensions and soil properties are presented in Table 1 as well. Ground water is not considered in this model, but for special case design, it can be involved. The interface of soil and lining has the same type of soil with a 0.83 reduction coefficient in strength parameters (C , ϕ), which leads to a 0.7 reduction coefficient in shear modulus (Pasdarpour and Vahdani 2012). Relative displacements along the interface are allowed in the tangential direction, and in the normal direction, a hard contact is assigned. Moreover, the separation of tunnel lining and soil is allowed after contact. In this paper, soil shear modulus is assumed to be constant as mentioned in Table 1, while in practical pushover analyses it can be assumed as a function of soil strain (Kramer 1996). Such a model can be built in geotechnical FEM software like PLAXIS 2D-8.5 (2006).

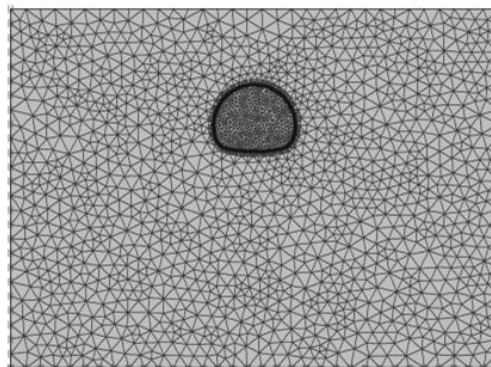


Figure 2: 2D static FEM model

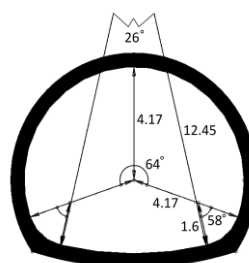


Figure 3: Dimensions of three-arch final lining

Table 1: Final lining and soil deposit parameters

Symbol	Soil parameters	Final lining parameters
E (KN/m ²)	1.5*10 ⁶	2.48*10 ⁷
G (KN/m ²)	5.77*10 ⁵	-
ρ (Kg/m ³)	1700	2400
ν	0.3	0.15
Height (m)	38	7.875
Width (m)	50	9.35
ϕ (°)	20	-
ψ (°)	1	-
C (KN/m ²)	10	-
Cs (m/s)	576.7	-
Lining Thickness (m)	-	0.5

* Lining dimensions are from outer side of the lining. Tunnel overburden depth is 8 meters. Height and width of soil deposit is used for the model initial dimensions and they will change in step 2.

Step 2: Loading and model dimensions determination

The load combination used for seismic analysis is based on equation (1) proposed by Wang (1993) for the MCE level of hazard and bored or mined tunnel. This equation simply adds all possible stresses all together. Since pushover analysis is nonlinear and static, all loads with their coefficients in load combination must be applied in one model.

$$U=D+L+EX+H+EQ, \quad (1)$$

where U is the required structural strength capacity, D is effects due to the dead loads of structural components, L is effects due to live loads, EX is effects of static loads due to excavation, H is effects due to hydrostatic water pressure and EQ is effects due to design earthquake motion. The first step for loading is the application of gravity (dead load of soil and on-ground structures) to the non-perforated FEM model. The next step is the assignment of the cavity to the model. Meanwhile, some parts of unbalanced forces in the boundary of the cavity can be released in the form of displacement, representing the relaxation process. Then, the lining is placed and the rest of unbalanced forces (EX and H) can be released together with the application of live load (L) and dead load of structural components (D). In this modeling practice, relaxation is ignored and all the unbalanced forces are transmitted to linings. Now, in order to gain better results from the FEM model, the two side boundaries are extended as much as the stresses in these boundaries find a triangle form and the effect of tunnel presence decays in the boundaries (Pasdarpour and Vahdani 2012).

To consider the effect of an earthquake on lining structures (EQ), the box of soil is pushed over by a static triangle prescribed horizontal displacement, which is applied to both sides of the model simultaneously as seen in Figure 4. In this regard, any shape of displacement such as the parabolic one can be applied to the both boundaries. It is better to choose a displacement shape, which is more similar to the fundamental vibration mode of the model. In addition, body forces (e.g. in the form of seismic coefficient multiplied by the layers mass, FHWA 2009) can be applied to the model as seismic loading. In order to use pushover analysis in actual engineering practice, soil stiffness and strength parameters should change before applying seismic prescribed

displacement. Although dynamic and static properties of soil are different, here they are assumed equal both in pushover analyses and the time history analyses performed for evaluation in section 3; hence, for the method investigation purposes, the assumption is correct.

The amount of the horizontal prescribed displacement on the ground surface is 503 mm as seen in Figure 4. Therefore, the mean ground shear strain equals the horizontal prescribed displacement divided by the model height, which is 0.0132. In the mean ground shear strain, the plastic points of the model are observed in the cases of presence and absence of the tunnel. The boundaries are extended so that the overall patterns of plastic points in the presence of the tunnel compared to the absence of it have fewer changes. On the other hand, the smallest dimensions with this aforementioned quality must be selected because otherwise the pattern of plasticity for very big dimensions would be incorrect (Pasdarpour and Vahdani 2012). Eventually, the height of 40 m and the width of 66 m have been achieved and illustrated in Figure 5.

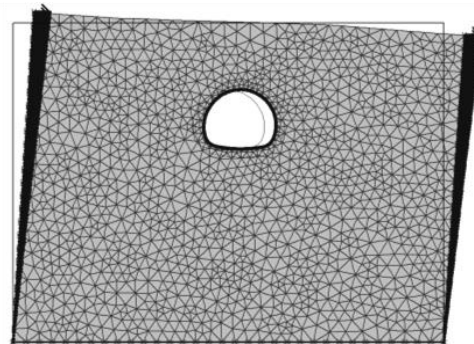


Figure 4: Static model under prescribed triangular displacement on both sides

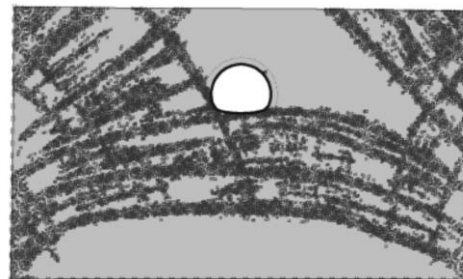


Figure 5: Plastic points in final dimensions after seismic loading

Step 3: Calculating capacity and force curves and converting them

Horizontal displacements of the top and bottom of the lining in the outer side of the tunnel are extracted during the application of prescribed seismic displacement. By subtracting these two displacements from each other, the tunnel racking (R_{TT}) is obtained. The prescribed triangular displacement is similar to the building lateral load in its pushover analysis as seen in Figure 1 and the building roof displacement is similar to the ground surface displacement. In ordinary pushover analysis, the building base shear force is the vertical axis of capacity so that it can be converted to the roof acceleration by dividing it by the building mass. On the other hand, the building roof acceleration is equal to the ground surface acceleration and the tunnel drift is a function of the ground surface acceleration (Power et al., 1998, Hashash et al., 2006). Thus, the building base shear force is similar to the tunnel drift. The resultant capacity curve is the tunnel drift (D_{TT}), which is equal to the tunnel racking divided by the tunnel height, versus the mean ground shear strain (γ_T), which is the ground surface horizontal displacement divided by the model height, as shown in Figure 6.

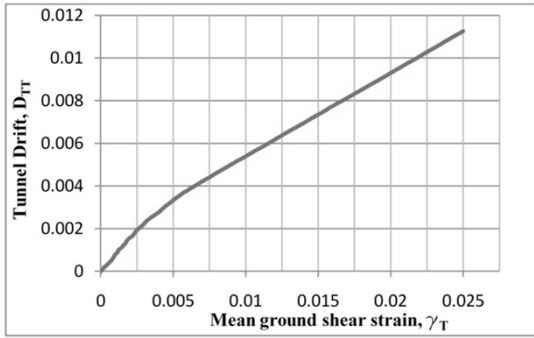


Figure 6: Capacity curve

In most cases, the capacity curve has two slopes. The first slope relates to the elastic behavior of the whole model in which plastic points are not dominant in the model behavior. The second slope relates to the plastic behavior of the whole model in which plastic points form a series of slices in the model during the seismic loading process. The total horizontal force required for the application of the prescribed triangular seismic displacement on both boundaries is extracted during the seismic loading.

This horizontal force is exactly the same as the base shear force in the ordinary pushover analysis. The force curve is the total horizontal force versus the mean ground shear strain as presented in Figure 7.

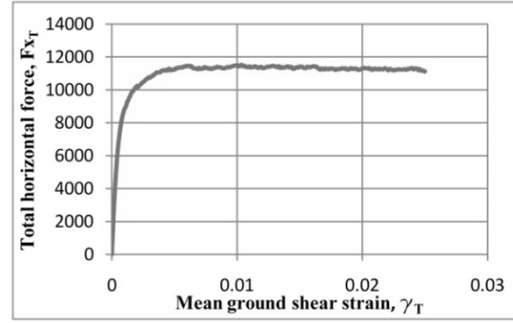


Figure 7: Force curve

This capacity and force curve is for multi-degree of freedom system (MDOF). However, in pushover analysis they must be changed to their equivalent SDOF system ones. Having converted MDOF to SDOF, the horizontal and vertical axes of the current capacity and force curve should be multiplied by coefficients based on structural dynamics (ATC 40, 1996). To convert the horizontal axis to a SDOF system, we use equation (2) as follows:

$$\gamma = \gamma_T / (PF_1 \times \phi_1), \quad (2)$$

where γ is the mean ground shear strain of an equivalent SDOF system, ϕ_1 is the amplitude of the first mode at the roof (ground surface) level and PF_1 is the modal participation factor for the first mode, which is obtained from equation (3):

$$PF_1 = \frac{\left[\sum_{i=1}^N (m_i \times \phi_{i1}) \right]}{\left[\sum_{i=1}^N (m_i \times \phi_{i1}^2) \right]} = \frac{\left[\int_0^H \phi_{y1} \times dy \right]}{\left[\int_0^H \phi_{y1}^2 \times dy \right]} = \frac{3}{2}, \quad (3)$$

where N is the level of N , which is the uppermost in the main portion of the model, m_i is the mass assigned to level i and ϕ_{i1} is the amplitude of the first mode at level i . By considering that the mass is distributed uniformly in height, and the shape of the first mode of vibration is triangular under the maximum value equals to one at the ground level (

$\phi_1 = 1$), the result will be according to equation (3):

Moreover, the vertical axis of both the capacity and force curves must be divided using equations (4) and (5):

$$D_T = D_{TT} / \alpha_1 \tag{4}$$

$$F_X = F_{XT} / \alpha_1 \tag{5}$$

where, D_T and F_X are the tunnel drift and total horizontal force in the equivalent SDOF system respectively. α_1 is the effective mass coefficient for the first mode, which is calculated using equation (6). All parameters in this equation have previously been defined.

$$\alpha_1 = \frac{\left[\sum_{i=1}^N (m_i \times \phi_{i1})^2 \right]}{\left[\sum_{i=1}^N (m_i) \sum_{i=1}^N (m_i \times \phi_{i1}^2) \right]} = \frac{\left[\int_0^H \phi_{y1} \times dy \right]^2}{\left[\int_0^H dy \times \int_0^H \phi_{y1}^2 \times dy \right]} \tag{6}$$

$$= \frac{3}{4}$$

By applying these coefficients to both axes of the capacity and force curves in Figures 6 and 7, the eventual capacity and force curves of the equivalent SDOF system using only the first mode of vibration are obtained as represented in Figures 8 and 9, respectively. This capacity curve must intersect a demand curve in the same coordinates. These coordinates for the capacity curve have the ability of observing the tunnel performance during ground movements. Moreover, the force curve of the equivalent SDOF system, as shown in Figure 9, will be utilized to calculate the damping coefficient of the model.

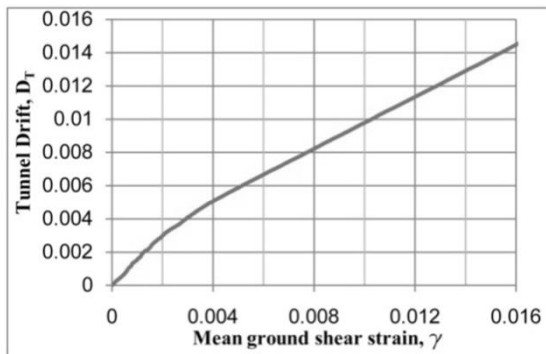


Figure 8: Capacity curve of the equivalent SDOF

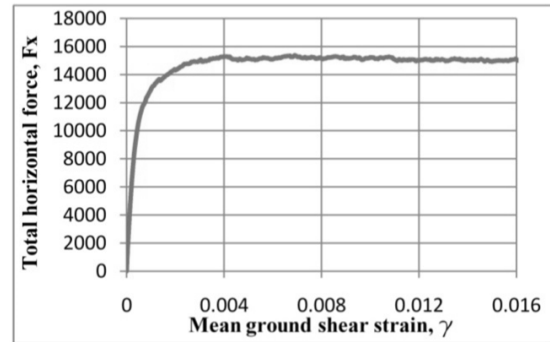


Figure 9: Force curve of the equivalent SDOF

Step 4: Choosing an earthquake, guessing a performance point due to it and calculating the damping of the model in the assumed performance point

To evaluate the seismic performance of a tunnel in pushover analysis, a demand curve must be used to intersect the capacity curve. Seismic demand curve sources can be a specific earthquake or a standard spectrum, which represents a standard earthquake. In this section, in order to introduce the method of pushover analysis, the El Centro earthquake has been used primarily to obtain the demand curve whose parameters is shown in Table 2 (The PEER 2011). The value of forces and deformations of the three-arch tunnel lining due to this earthquake is obtained using pushover analysis.

Table 2: El Centro earthquake parameters

Symbol	Quantity
Magnitude (Mw)	7.1
PGA (g)	0.319
PGV (cm/sec)	35.738
PGD (cm)	20.5
Preferred (m/s)	766.80
Predominant period (s)	0.5

* El Centro, California, USA, 1940-5-18, Longitudinal

Over the current step, a performance point must be guessed as an assumed probable answer of pushover analysis. Performance point of the tunnel lining due to any seismic excitation such as the El Centro earthquake is the earthquake maximum

effect and can be expressed in terms of a point on the capacity curve with a mean ground shear strain. For the first try, a performance point equal to $\gamma=0.0016$ was assumed as the probable performance point due to the El Centro earthquake. Now, the damping coefficient of the model in this assumed performance point can be calculated using the force curve of the equivalent SDOF system in Figure 9. To calculate the damping coefficient using this curve, a bilinear form of it must be derived for the assumed performance point (ATC 40 1996, 360 No 2005). In order to obtain a bilinear curve for a certain performance point, a total horizontal force is supposed as a yield force (F_{xy}) of the model. Then, the first line must pass the force curve at $F_x=0.6 \cdot F_{xy}$. The first point of the second line is the yield point on the first line. The second point of the second line is the assumed performance point on the main force curve. The yield force must be chosen as if the area below the bilinear and the main force curves be the same with an accuracy of 1 percent. According to Figure 10 and Table 3, for the assumed performance point, the total horizontal force at the yield point is 11200 KN.

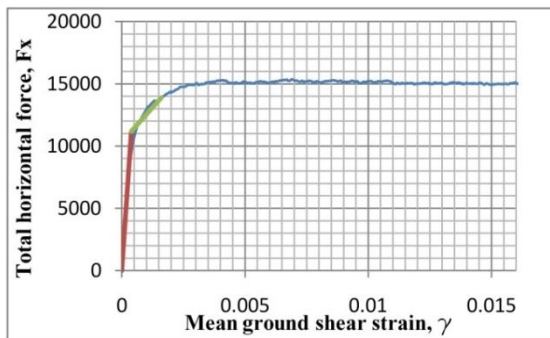


Figure 10: Bilinear form of equivalent SDOF force curve

Table 3: Areas of the force curves

Symbol	Quantity
Performance point (γ)	0.0016
Bilinear force curve area	17.416
Main force curve area	17.3347
difference	4.69E-01%
allowable	1%

Two essential parameters for calculating the damping coefficient are α and β , which both are the

parameters of the model bilinear force curve in a certain performance point as shown in equations (7) and (8). They represent the model hysteresis loop parameters with triangular loading.

$$\alpha = \frac{\text{slope of second line}}{\text{slope of first line}} \tag{7}$$

$$\mu = \frac{\gamma \text{ at performance point}}{\gamma \text{ at yield point}} \tag{8}$$

Now, the damping coefficient (β_{eff}) can be calculated for a given performance point by equation (9) (ATC 40 1996, 360 No 2005).

$$\beta_{eff} = 0.05 + K \frac{2 (\mu - 1)(1 - \alpha)}{\pi \mu(1 + \alpha\mu - \alpha)} \tag{9}$$

where K is a coefficient for assessing deterioration in the model hysteresis loop so that its value is dependent on the value of β_0 , which is calculated from equation (10) (See Tables 4 and 5).

$$\beta_0 = \frac{2 (\mu - 1)(1 - \alpha)}{\pi \mu(1 + \alpha\mu - \alpha)} \tag{10}$$

Table 4: Value of K (ATC 40)

Structural behavior type	β_0	K
Type A	<0.1625	1
	>0.1625	$1.13 - 0.51(\pi / 2)\beta_0$
Type B	<0.25	0.67
	>0.25	$0.845 - 0.446(\pi / 2)\beta_0$
Type C		0.33

Table 5: Type of structure (ATC 40)

Shaking Duration	Essentially new building	Average existing building	Poor existing building
Short	Type A	Type B	Type C
Long	Type B	Type C	Type C

Values presented in Tables 4 and 5 are for buildings, but in the absence of real data for the

model of a tunnel and soil, they may be used. Based on ATC 40, an earthquake with the magnitude of more than 6.5 M_w , (e.g. El Centro earthquake) in seismic zone type 4, which is the pre-assumed seismic zone in this work, must be considered as a long period ground shaking. In addition, by defining the structure considered in this study as a new building, the type of the structure will be Type B according to Table 5. As a result, the damping coefficient in the assumed performance point using equation (9) is:

$$\left\{ \begin{array}{l} \alpha = 0.07601 \\ \mu = 4.173 \end{array} \right. \Rightarrow \beta_0 = 0.36036 > 0.25$$

$$\Downarrow$$

$$\beta_{eff} = 0.26353 = 26.353\%$$

Step 5: Calculating acceleration response spectrum

In the process of calculating the demand curve, the record of the El Centro earthquake is primarily given to the SEISMOSIGNAL program and the acceleration response spectrum of an elastic SDOF system with the damping coefficient obtained from the last step is calculated as shown in Figure 11. In fact, the acceleration response spectrum of the El Centro earthquake was reduced by 26.4% viscous damping, which is the model damping in the assumed performance point.

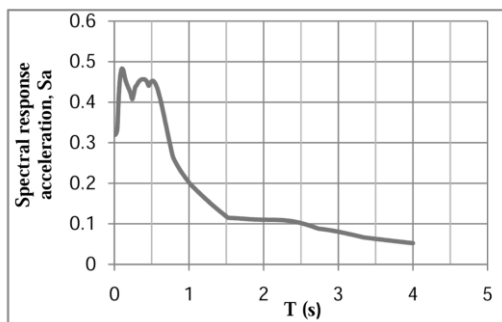


Figure 11: El Centro acceleration response spectrum with 26.4% damping

Step 6: Converting acceleration response spectrum to demand curve

To intersect the tunnel capacity and the demand curves, the axes of these curves must be the same. Consequently, in order to obtain the demand curve, the horizontal and vertical axes of the El Centro

acceleration response spectrum (Figure 11) as demand spectrum will be converted to the horizontal and vertical axes of the capacity curve (Figure 8). It is notable that this demand curve will be free-field demand for a SDOF system.

• **Converting vertical axis**

The vertical axis of earthquake acceleration response spectrum is converted to the free-field shear strain of soil at the depth of the tunnel, which is equal to the tunnel drift in the capacity curve vertical axis. Hence, this shear strain will be free-field demand for tunnel lining analysis (Hashash 2006). Initially, the vertical axis, which is maximum spectral acceleration response on the ground surface, is converted to the peak ground velocity using Table 6.

Table 6: Ratio of peak ground velocity to peak ground acceleration at surface (after Power et al., 1996)

Moment Magnitude (M_w)	Ratio of peak ground velocity(cm/s) to peak ground acceleration (g)		
	Source-to-site distance (km)		
	0-20	20-50	50-100
Rock*			
6.5	66	76	86
7.5	97	109	97
8.5	127	104	152
Stiff soil*			
6.5	94	102	109
7.5	140	127	155
8.5	180	188	193
Soft soil*			
6.5	140	132	142
7.5	208	165	201
8.5	269	244	251

*in this table the sediment types represent the following shear wave velocity range: Rock >750 m/s; stiff soil is 200-750 m/s; and soft soil <200 m/s. the relationship between peak ground velocity and peak ground acceleration is less certain in soft soil.

Based on El Centro earthquake, the magnitude of $M_w=7.1$ and the source to site distance of 20-50 (Km) are assigned and due to the shear wave velocity in model soil the stiff soil is allocated.

Accordingly, the coefficient of 117 must be multiplied to each point of the acceleration response spectrum vertical Axis. Then, the peak ground velocity is converted to the peak velocity at the depth of the tunnel using Table 7, of course in the absence of detailed data for this coefficient.

Table 7: Ratio of ground motion at depth to motion at ground surface (after Power et al., 1996)

Tunnel depth (m)	Ratio of ground motion at tunnel depth to motion at ground surface
6	1.0
6-15	0.9
15-30	0.8
> 30	0.7

The model overburden is 8 m, and the depth to centre of the tunnel is 12.75 m approximately. Therefore, coefficient of 0.9 must be multiplied to each point of the spectrum vertical axis to gain the peak velocity of particles at the depth of the tunnel. Then, according to equations (11) and (12), by dividing each point of the vertical axis to the shear wave velocity of soil, the free-field shear strain at the depth of the tunnel or vertical axis of demand curve will be calculated (Newmark 1968). Where, γ and V_s are the free-field shear strain and horizontal particle velocity at the depth of the tunnel, respectively. In addition, C_s , ρ and G are the shear wave velocity, density and shear modulus of soil, respectively.

$$\gamma = \frac{V_s}{C_s} \quad (11)$$

$$C_s = \sqrt{\frac{G}{\rho}} \quad (12)$$

• Converting horizontal axis

The horizontal axis of earthquake acceleration response spectrum is converted to the mean ground shear strain, which is the same horizontal axis of capacity curve. The soil box without the tunnel is considered as SDOF, therefore by considering a hypothetical natural period for the box in the horizontal axis of the earthquake acceleration response spectrum, the ground surface displacement due to the earthquake can be obtained using equation (13) (ATC 40 1996).

$$S_d = S_a \times \frac{T^2}{4 \times \pi^2} \quad (13)$$

Where S_a and S_d are the maximum acceleration response and displacement of a SDOF system with a natural period of T due to the earthquake. By assuming the soil box elastic in the demand curve and the strain of the ground as a free-field strain, the mean ground shear strain (Horizontal axis of demand curve) is calculated using equation (14), in which H is the height of the model. The result of converting both axes of the earthquake response spectrum is the demand curve as shown in Figure 12.

$$\gamma = \frac{S_d}{H} \quad (14)$$

Step 7: Interacting the capacity and demand curves

The equivalent SDOF capacity curve is provided in Figure 8 and by intersecting it with demand curve, as seen in Figure 12, properties of the intersection point were attained. At the intersection point, mean ground shear strain of SDOF system (γ) is 0.0016 and tunnel drift of SDOF system (D_T) is 0.00248.

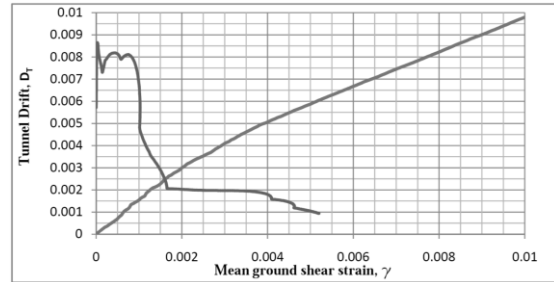


Figure 12: Intersection of Capacity curve with Demand curve from El Centro earthquake

Step 8: Verifying the interaction point as a performance point

If the intersection point of capacity and demand curves is the assumed performance point with a maximum difference of 1%, then the intersection point will be the correct performance point (ATC 40 1996). Otherwise, another performance point must be assumed in step 4, and then, steps 4

through 8 must be repeated. In this example, the assumed performance point for the El Centro earthquake was $\gamma=0.0016$ and the two curves intersection point is the same according to Figure 12, therefore, the assumption was correct.

Step 9: calculating forces/moments and rotations in the performance point

The performance point, which is verified in Step 8, is indeed the intersection point of the demand curve and equivalent SDOF capacity curve; thus, it is an equivalent SDOF system performance point. In this step, in order to attain lining forces/moments and rotations in the calculated performance point, it is needed to convert the equivalent SDOF system performance point to the main model one, which is MDOF system using step 3 reversely. Here, the calculations are presented and the model performance point details due to the El Centro earthquake are given in Table 8.

$$\begin{cases} \gamma_T = \gamma \times PF_1 = 0.0016 \times 3/2 = 0.0024 \\ D_{TT} = D_T \times \alpha_1 = 0.00248 \times 3/4 = 0.00187 \\ D_g = \gamma_T \times H = 0.0024 \times 4000 = 9.6\text{cm} \\ R_{TT} = D_{TT} \times H_T = 0.00187 \times 787.5 = 1.473\text{cm} \end{cases}$$

Table 8: El Centro performance point details

Symbol	Quantity
Mean ground shear strain of SDOF, γ	0.0016
Tunnel drift of SDOF, D_T	0.00248
Mean ground shear strain of model, γ_T	0.0024
Tunnel drift of model, D_{TT}	0.00187
Ground displacement of model, D_g (cm)	9.6
Tunnel racking of model, R_{TT} (cm)	1.473
Effective fundamental period, T_{eff} (s)	1.36

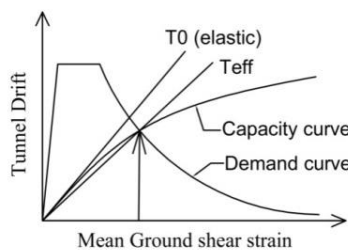


Figure 13: Effective fundamental period

The model effective fundamental period of vibration (T_{eff}) in Table 8 (ATC 40 1996) is indeed natural vibration period of equivalent SDOF system in performance point which was calculated 1.36s by acting based on step 6 inversely. Note that this period has considered both the soil nonlinear behavior and the tunnel effect. Therefore, unlike the elastic one (T_0) in Equation 23, it depends on the demand earthquake as the model nonlinear behavior intensity will vary by earthquake characteristics (See Figure 13). Pushing the model up to the performance point, which is displacement of 9.6 cm on the ground surface, maximum lining pressure force is -1278.9 KN, maximum shear force is 400.25 KN and maximum moment is -647.19 KN*m. Since lining in this example is defined elastically, only forces/moments are important and linear analysis criteria must be used for checking them. However, if lining is assigned inelastic, rotations of predefined or engendered hinges can be obtained in the performance point and under this condition, nonlinear analysis criteria must be then utilized. Nine steps of pushover analysis using a record of an earthquake and calculating the performance point are summarized as follows:

1. Build a nonlinear 2D FEM model of soil and the tunnel using a software like PLAXIS 2D.
2. Load the numerical model and determine the dimensions of it during the loading process.
3. Extract the capacity curve and force curve from loading process. Then convert them to their equivalent SDOF system type.
4. Choose an earthquake and assume a performance point for it. Afterward, calculate the damping coefficient of the model in the assumed performance point using the force curve.
5. Obtain the earthquake elastic acceleration response spectrum using the damping coefficient of the previous step by the SEISMOSIGNAL program.
6. Convert the axes of earthquake acceleration response spectrum to the axes of demand curve.
7. Intersect the consequent demand curve with the equivalent SDOF capacity curve.
8. If the intersection point is equal to the assumed performance point with 1% difference, it is the earthquake correct performance point. Otherwise turn back to step 4 and choose another more probable

performance point and repeat Steps 4 through 8.

- Having the resultant SDOF performance point, calculate its equivalent performance point for the main MDOF model and obtain forces/moments or hinges rotations of lining in this final performance point.

These nine steps were then performed for three other earthquakes. The earthquakes parameters are introduced in Table 9 and the results of their pushover analyses are shown in Table 10 and Figure 14. It is remarkable that the source to site distance in Table 9 is the average of Campbell and Jooyner distances (FEMA P695 2009).

Table 9: Earthquakes parameters

Symbol	Kocaeli	Manjil	Tabas
Magnitude (M_w)	7.5	7.4	7.35
PGA (g)	0.219	0.515	0.836
PGV (cm/sec)	17.57	42.41	97.717
PGD (cm)	16.21	15.02	38.54
Preferred (m/s)	523	724.0	766.80
Predominant period (s)	0.16	0.16	0.24
Source to site distance (km)	12.05	12.8	4.285

*Kocaeli, Arcelik, Turkey 1999, Longitudenal

*Manjil, Abbar, Iran 1990-06-20, Longitudenal

*Tabas, Tabas, Iran 1978-09-16, Longitudenal

Table 10: Earthquakes performance points details

Symbol	Kocaeli	Manjil	Tabas
γ	0.00068	0.00172	0.0058
D_T	0.00106	0.00262	0.00649
γ_T	0.00102	0.00258	0.0087
D_{TT}	0.000795	0.00197	0.00487
D_g (cm)	4.08	10.32	34.8
R_{TT} (cm)	0.6261	1.5514	3.8351
T_{eff} (s)	1.08	1.467	1.718

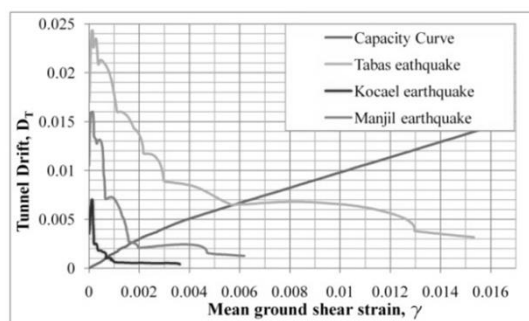


Figure 14: Earthquake performance point

2.2. Pushover analysis using a standard demand

The aim of this section is to illustrate how to use a typical standard acceleration response spectrum representing a standard earthquake in pushover analysis of a tunnel (Pasdarpour and Vahdani 2012). A design base level standard acceleration response spectrum of a model consisting of soil and tunnel is illustrating its elastic response to a design base level earthquake. Such a spectrum has to consider soil deposit seismic amplification and lining design considerations at least for various types of soil and lining. However, in the absence of such a spectrum, buildings' standard acceleration response spectrum, obtained from a building seismic manual (such as FEMA 302), may be utilized. Indeed, it was assumed that the response of the model of soil with tunnel to a standard earthquake corresponds almost to a building response, which was drawn in buildings' standard spectrum. Note that the accuracy of this assumption is not a matter of disputation, because the aim in this section was just using a typical spectrum and illustrating the ability of pushover analysis to employ it. For example, we want to perform pushover analysis on a tunnel with the same properties presented in Figure 3 and 2 in Moncks Corner of South Carolina in the USA using buildings' standard spectrum of FEMA 302 for design base level earthquake. Pushover analysis with a standard spectrum is similar to pushover analysis with an earthquake spectrum, which was summarized in nine steps, with only differences in steps 4 and 5, so we skip repeating Steps 1 through 3.

In Step 4, it is needed to calculate a standard response spectrum based on FEMA 302 provisions.

To calculate the standard spectrum, two spectral accelerations of one and the short period due to the maximum considered earthquake at the bottom boundary of the static model (40 meters under ground level) in the site of tunnel construction must be calculated based on ASCE 7 maps (2005). Because of the hypothetical nature of this example, these values are selected near the real values in maps of southern Carolina next to Moncks Corner:

$$S_1 = 0.825 \text{ (g)} \quad \text{for } T=1$$

$$S_s = 1.3125 \text{ (g)} \quad \text{for short period}$$

In order to calculate standard spectrum, the soil type below the model bottom boundary or below 40 meters must be determined which in this example is assumed the same type of model soil, that is C due to its shear wave velocity equal to 576.7 (m/s). Using the relationships of FEMA 302, the ultimate standard response spectrum for the design base level is obtained, as presented in Figure 15 (top-left). Now, a performance point must be assumed for this demand and the model-damping coefficient in this point can be calculated using equation (9). Note that a hypothetical earthquake, corresponding the FEMA 302 spectrum in the

design base level, is supposed to have a magnitude of more than 6.5 M_w . Hence, this hypothetical earthquake is a long period one and the type of structural behavior is B, according to Table 5.

$$\gamma_{pp} = 0.00282 \Rightarrow \beta_{eff} = 0.2823$$

Then and in Step 5, reduction coefficients, SRV and SRA, will be calculated for an assumed performance point through equations (15) and (16) (ATC 40 1996, 360 No 2005). The $SRA=0.4427$ is multiplied to the acceleration fixed part of the standard spectrum and the $SRV=0.5699$ is multiplied to the velocity fixed part of it. The resultant reduced standard spectrum is presented in Figure 15 (top-right).

$$SRA = \frac{3.21 - 0.68 \ln(100\beta_{eff})}{2.12} \tag{15}$$

$$SRV = \frac{2.31 - 0.41 \ln(100\beta_{eff})}{1.65} \tag{16}$$

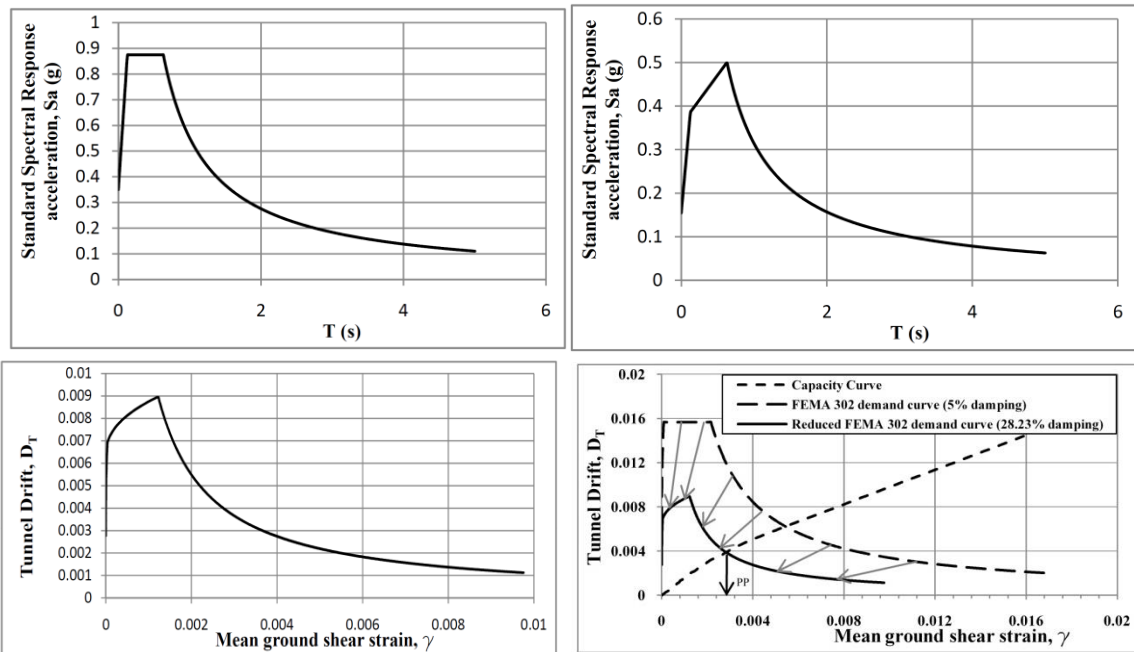


Figure 15: Based on FEMA 302: Standard acceleration response spectrum (top-left), reduced standard acceleration response spectrum (top-right), reduced demand curve (bottom-left) Performance point (bottom-right)

The remaining steps are the same previous section ones. For step 6, converting demand axes, the selected region in this example is near the source of the earthquake; hence, the source to site distance of 0-20Km is assigned (see ASCE 7 maps). In addition, a magnitude of 7 Mw is chosen because the spectrum is for the design base level. The results of converting the axes are illustrated in Figure 15 (bottom-left). By intersecting the reduced demand curve with the capacity curve in Step 7, the intersection point will be obtained like Figure 15 (bottom right) and Table 11. Furthermore, in Figure 15 (bottom-right), a non-reduced demand curve or demand curve with 5% damping is presented to illustrate the reduction process effect. The obtained intersection point is equal to the assumed performance point, thus in step 8 the point is verified as the correct performance point. Note that all possible non-seismic loads such as dead, live, etc. are applied to this static model according to load combination of equation (1) before pushing over it. Consequently, it is not needed to perform additional analysis to add effects of other loads to the seismic load one.

Table 11: Performance point details with FEMA 302 demand

Symbol	Quantity
γ	0.00282
D_T	0.00387
γ_T	0.00423
D_{TT}	0.002903
D_g (cm)	16.92
R_{TT} (cm)	2.286
T_{eff} (s)	1.43

3. Evaluation of the pushover analysis method with dynamic time history analysis

In order to evaluate the results of pushover analyses with an earthquake demand presented in Tables 8 and 10, nonlinear dynamic analysis was utilized. In dynamic analyses, the same Mohr-coulomb plain strain model as presented in step 1 of section 2.1, with a height of 50 m and a width of 80 m was built as shown in Figure 16. Compared with the pushover analysis model the width of the dynamic model was increased in order to decrease the effect

of boundaries on the tunnel behavior during dynamic analysis. Likewise, its height has been chosen based on equation (17) in which Ave(T_d) is the earthquakes average predominant period equals to 0.265 s.

$$H > \frac{Ave(T_d) \times C_s}{4} = 38.2 \quad (17)$$

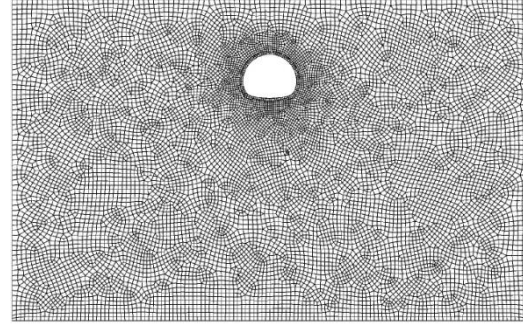


Figure 16: Dynamic 2D FEM model

After applying the gravity, the velocity of the earthquakes, presented in Tables 2 and 9, was applied to the model bottom boundary as the velocity of base stone. There are dashpots (dampers) and springs at the two-side boundaries of the model and just dashpots at the bottom boundary of it for modeling half-infinite space and building absorbent boundaries. Their specifications are based on equations. (18)-(22) (PLAXIS manual, 2006).

$$F_d = C_d \cdot u \quad (18)$$

$$C_d = \rho \cdot V_p \cdot A \quad \text{For two side boundaries} \quad (19)$$

$$C_d = \rho \cdot V_s \cdot A \quad \text{For bottom boundary} \quad (20)$$

$$F_k = k \cdot u \quad (21)$$

$$k = \frac{E}{H \cdot (1 - \nu^2)} \cdot A \quad (22)$$

where F_d and F_k are dashpot and spring forces, respectively, C_d is the damping coefficient, K is spring stiffness, A is the area of each dashpot or spring, and V_p and V_s are the velocities of pressure and shear wave in soil, respectively, which are obtained from elasticity. Other parameters have been introduced before. The Interface between soil and the tunnel is the same as the pushover model one as stated in Step 1. Rayleigh damping parameters of soil (α , β) were assigned 0.01 and soil structural damping was 0.05 in dynamic model (Pasdarpour and Vahdani 2012). Such a dynamic

model can be built in FEM software such as ABAQUS (ABAQUS User's manual, 2002).

Tunnel racking measured from outer boundary of lining during El Centro earthquake is demonstrated in Figure 17. The results of all dynamic analyses and their differences with pushover analyses ones are illustrated in Table 12. As seen, in all cases pushover analyses have evaluated tunnel racking less than dynamic analyses, while ground surface displacements have been estimated more using pushover analyses than dynamic analyses. Apparently, this difference can be originated chiefly from the natural error of pushover analysis resulted from converting a MDOF system to an equivalent SDOF system. If the fundamental mode of vibration is not so dominant, pushover analysis will not evaluate the MDOF system performance well enough as it happens in tall buildings analysis (Krawinkler et al., 1998). In this case, evaluated roof displacements (equal to ground surface displacements) are usually over but evaluated accelerations/forces, which represent the tunnel drift, are less than dynamic results as it happened in Table 12. Thus, when the tunnel dimensions are big, the whole model is consequently similar to a tall building; and alternatively modal pushover analysis may be utilized to consider the effect of higher modes of vibration in these cases (Chopra et al., 2002). To conclude, having averagely 13.25% difference of lining racking with dynamic analysis, the method of pushover analysis is verified for seismic assessment of shallow tunnel constructed in soil.

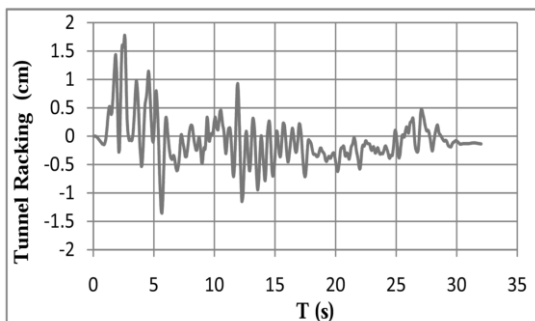


Figure 17: Dynamic response to El Centro earthquake

Table 12: Maximum tunnel racking and displacement of ground surface due to dynamic analyses (cm)

Earthquake	Kocaeli	El Centro	Manjil	Tabas
R_{TT} (Dynamic)	0.75	1.7767	1.8279	4.018
R_{TT} (Pushover)	0.6261	1.473	1.5514	3.8351
R_{TT} Difference	16.52%	17.1%	15.13%	4.55%
Dg (Dynamic)	4.4	8.8	7.51	22.25
Dg (Pushover)	4.08	9.6	10.5	34.8
Dg Difference	7.27%	-7.71%	-39.8%	-56.4%

In continue, although the purpose of pushover analysis using FEMA building spectrum in section 2.2 was just showing the method of using a typical standard spectrum, the results of it (Table 11) will also be evaluated by means of nonlinear dynamic analysis to see how much they are near to real response of the tunnel. The same dynamic analysis will be executed by choosing seven earthquakes from far-field record sets of FEMA P695. Characteristics of these seven earthquakes are presented in Table 12. Six of them have the soil type C beneath their recorders, which is the same soil type of the main model and the beneath soil type of the last record is D. In addition, six of these earthquakes have the source to site distance of 0-20Km, which is similar to the assumption made in Section 2. These earthquakes must be normalized and scaled to the standard spectrum in Figure 15 (top-left) and then be applied to the bottom boundary of the dynamic model. The height of the model is checked with Equation (17) again for earthquakes in Table 13.

Table 13: Chosen earthquakes from far-field set of FEMA P695

EQUATION	Characteristics (Longitudinal)	Mag. (M _w)	PGA (g)	PGV (cm/s)	PGD (cm)	Preferred V _{s30} (m/s ²)	Source to site distance (Km)	Dominant period (s)
Manjil	Manjil, Abbar, Iran 1990-06-20	7.37	0.505	43.78	18.96	724	12.8	0.16
Kobe	kobe, Nishi-Akashi, Japan 1995	6.9	0.509	37.097	18.96	609	16.15	0.46
Chi Chi	ChiChi, TCU045, Taiwan 1999	7.6	0.474	36.7	50.7	705	26.4	0.44
Kocaeli	Kocaeli, Arcelik, Turkey 1999	7.5	0.219	17.695	13.7	523	12.05	0.16
Friuli	Friuli, Tolmezzo, Italy 1976	6.5	0.351	22.037	4.1	425	15.4	0.26
Hector	Hector Mine, Hector, USA 1999	7.1	0.266	28.557	22.5	685	10.4	0.22
Northridge	Northridge, Beverly Hills-Mulhol, USA 1994	6.7	0.416	58.948	13.1	356	9.4	0.52

In FEMA P695, the normalization process is conducted using PGV with factors presented in Table A-4D. Moreover, the FEMA scaling process makes the average spectral acceleration response with 5% damping of all seven earthquakes more than the manual spectral acceleration response in the period of 0.2 T up to 1.5 T by multiplying a scaling factor to the earthquakes records (ASCE 7 2005). T is the fundamental period of the soil-tunnel model and in its elastic behavior domain is the predominant natural period of a shear wave in the elastic soil deposit (Dobry et al., 1976). Idriss and Seed (1968) have recommended equation (23) for this period.

$$T_0 = \frac{4 * H}{C_m} = 0.3468 \approx 0.35s \quad (23)$$

Where, H is the thickness of the soil deposit. The calculated scaling factor to be applied on the records is 1.2818. Ultimate normalized and scaled records of earthquakes are applied to the bottom boundary of the 2D dynamic model and the results are illustrated in Table 14. Although FEMA standard spectrum is for predicting seismic response of a building, six percent error in Table 14 shows that pushover analysis using this spectrum could predict seismic response of this specific tunnel model (Figure 2) well enough. Hence, the main problem remains in finding an accurate standard spectrum by further investigations on, whether developing current studies on FEMA spectrum to all cases of soil and tunnel properties or introducing an entirely more suitable standard spectrum.

Table 14: Dynamic analyses results

Earthquake	Max. Tunnel racking (cm)
Manjil	1.8222
Kobe	2.086
Chi Chi	3.7
Kocaeli	2.0115
Friuli	1.119
Hector	2.5356
Northridge	3.78535
Average dynamic	2.437
Pushover analyses	2.286
Difference	6.196%

4. Conclusions

A new seismic assessment method for shallow tunnels, which is pushing over the 2D nonlinear FEM model, was introduced in section 2 using four earthquakes demand and the standard demand of FEMA 302. Then the method is evaluated in section 3 using nonlinear dynamic analysis. The results of evaluation showed 13% difference for pushover analysis using the earthquakes demand and 6% difference for pushover analysis using the standard demand, which means that the pushover analysis method is generally acceptable to be used instead of elaborate dynamic analysis. However, in order to generalize this conclusion to other cases of tunnel or to reduce the pushover method error, we suggest to perform the following researches:

- Formulation of the model damping coefficient (β_{eff}) in equation (9) must be investigated in order to consider natural damping effect of the infinite two sides boundaries and geotechnical damping parameters of soil (Rayleigh damping). Moreover, value of structural behavior type (K) in Table 4 and 5 must be calibrated for seismic behavior of the geotechnical model.
- Accuracy of pushover analysis method presented in section 2 can undergo further evaluation by changing geotechnical and structural parameters of model as follow. a) Set the soil shear modulus (G/G_{max}) as a function of soil strain. b) Choose various flexibility ratios, which are stiffness ratios of tunnel lining to soil. c) Apply various shapes of seismic prescribed displacement to the two side boundaries of the model, else than triangular shape such as parabolic one. d) Consider other soil and lining mechanical behavior type such as Hardening Soil and inelastic respectively. e) Use other tunnel cross-section geometry shapes such as rectangular. f) Examine various tunnel dimensions and depths, which lead to various dimensions of the whole model. g) Involve ground water effects in the model.
- It is strongly recommended to develop modal pushover analysis for assessing shallow tunnels with large spans or in soft soil in order to consider the geotechnical models higher modes of vibration and reduce the inherent error of the method (see section 3).
- For performing pushover analysis using a standard spectrum it is needed to propose a more reliable standard spectrum, which is suitable to the geotechnical nature of the model through further investigations. In this regard, if it is intended to use the same FEMA 302 or 450 (2006) standard spectrum for seismic assessment of shallow tunnels it will be necessary to prove their efficiency for all cases of soil and lining properties such as stiffness, dimension, etc.

5. References

- ABAQUS User's manual, (2002) Hibbit, Karlsson and Sorensen Inc., Pawtucket, RI
- ASCE 7-05, American Society of Civil Engineers, Minimum Design Loads for Buildings and Other Structures, 2005 Edition
- ATC Report No. 40, Applied Technology Council (Seismic Safety Commission, State of California, 1996) "Seismic Evaluation and Retrofit of Concrete Buildings", Vol. 1
- Chopra, Anil K. and Goel, Rakesh K. (2002) "A modal pushover analysis procedure for estimating seismic demands for buildings", Earthquake engineering and structural dynamics, 31:561–582 (DOI: 10.1002/eqe.144)
- Dobry, R., Oweis, I. and Urzua, A. (1976) "Simplified procedures for estimating the fundamental period of a soil profile", Bull. Seismol. Soc. Am. 66, Vol. 4, pp. 1293-1321
- FEMA P695, Federal Emergency Management Agency, Quantification of Building Seismic Performance Factors, 2009 Edition
- FEMA 302, Federal Emergency Management Agency, NEHRP recommended provisions for seismic regulations for new buildings and other structures, part 1, 1997 Edition
- FEMA 356, Federal Emergency Management Agency (2000), Pre-standard and Commentary for the Seismic Rehabilitation of Building
- FEMA 450, Federal Emergency Management Agency, NEHRP recommended provisions for seismic regulations for new buildings and other structures, part 1, 2006 Edition

Performance-Based Seismic Assessment of Shallow Tunnels using Pushover Analysis: pp.63-81

- FHWA, Technical Manual for Design and Construction of Road Tunnels-Civil Elements, chapter 13, Publication No NHI-09-010, march 2009
- Hashash, Y.M.A., Hook, J.J., Schmidt, B. and Tao, J.C. (2001) “Seismic design and analysis of underground structure”, Tunneling and Underground space Technology, Vol.16, pp. 247-293
- Huo, H., Bobet, A., Fernandez, G., Ramirez, J. (2006) “Analytical solution for deep rectangular structures subjected to far-field shear stresses”, Tunnelling and Underground Space Technology, 21, pp.613–625
- Idriss, I.M., Seed, H.B., (1968) “Seismic response of horizontal soil layers”, Journal of Soil Mechanics and Foundation Div., ASCE 94 (SM4), 1003-1031
- Kramer, S. (1996) “Geotechnical Earthquake Engineering”, Prentice-Hall, Upper Saddle River, Nj, USA
- Krawinkler, H. and Seneviratna, G. D. P. K. (1998) “Pros and cons of a pushover analysis of seismic performance evaluation”, Engineering Structures, Vol. 20, Nos 4-6, pp. 452-464
- Newmark, N.M. (1968) “Problems in wave propagation in soil and rock”, Proceedings of the International Symposium on Wave Propagation and Dynamic Properties of Earth Materials
- Owen, G.N. and Scholl, R.E. (1981) “Earthquake engineering of large underground structures”, Report no FHWA/RD-80/195, Federal Highway Administration and National Science Foundation.
- Pasdarpour M., Vahdani S. (2012) “New method for seismic evaluation of shallow three-arch tunnels with pushover analysis based on performance”, Proceedings of International Conference on Earthquake and Structural Engineering, ICESE 2012, Kuala Lumpur, Malaysia, February 19-21.
- Pasdarpour M., Vahdani S. (2012) “A comparison of FEMA 302 provisions with 2800 code for seismic evaluation of shallow tunnels based on performance”, Proceedings of World Tunnel Congress, WTC 2012, Bangkok, Thailand, May18-23
- Penzien, J. (2000) “Seismically included racking of tunnels linings”, Earthquake Engineering and Structure Dynamics, Vol. 29, pp. 683-691
- PLAXIS manual (2006), 2D-Version 8. Delf University of Technology & PLAXIS b.v., The Netherlands
- Power, M.S., Rosidi, D. and Kaneshiro, J. (1996) “Vol. III Strawman: screening, evaluation and retrofit design of tunnels”, Report Draft. National Center for Earthquake Engineering Research, Buffalo, New York
- Power, M., Rosidi, D., Kaneshiro, J. (1998) “Seismic vulnerability of tunnels-revisited In: Ozedimir, L., (Ed.)”, Proceedings of the North American Tunneling Conference, Elsevier, Long Beach, CA, USA.
- Seed, H.B., Whitman, R.V., (1970) “Design of earth retaining structures for dynamic loads” Proceedings of the ASCE Specialty Conference on Lateral Stresses in the Ground and Design of Earth Retaining Structures.
- Shake2000 User’s manual, Copyright Gustavo A. Ordonez, 2000-2011, a computer program for 1-D analysis of geotechnical earthquake engineering problems.

The Pacific Earthquake Engineering Research Center, (Copy write © 2005) 'The PEER NGA database',
<<http://peer.berkeley.edu/nga/search.html>> (Dec. 10, 2011)

Wang, J.N. (1993) "Seismic Design of Tunnels: A State of the Art Approach", Monograph 7, Parsons,
Brinkerhoff, Quade and Douglas Inc, New York

360 No., Iranian Instruction for Seismic Rehabilitation of Existing Buildings, 2005 Edition